

FORMATION OF A TWO-PHASE REGION DURING VAPORIZATION  
IN POROUS MEDIA

I. E. Azizov and V. M. Entov

UDC 532.564:519.63

A physically consistent model is constructed to describe vaporization in a water-saturated porous medium. Results are presented from a numerical analysis of a frontal model and a model with a two-phase region.

The mathematical description of processes involving phase transformations often leads to physical contradictions when done within the framework of the frontal approach, which is based on the hypothesis that there exists a phase transformation surface (front). For example, in the case of the crystallization of a binary melt, the frontal model leads to the phenomenon of "diffusional" supercooling and destabilization of the crystallization front [1, 2]. These contradictions can be eliminated in a more general theory which allows the formation of a two-phase region — a mixture of two different phases of the same substance, coexisting under conditions of thermodynamic equilibrium. A model with a two-phase region was first realized in the mechanics of frozen soils in [3].

Another approach is being developed in the theory of multiphase processes in porous media [4, 5]. This approach is based on the idea that the phase transformation of the pore fluid occurs over an extensive range of the temperature spectrum. The approach is based on experimental determinations of the phase composition from thermodynamic functions of state (state parameters). In this case, the diffusion equation of the pore moisture is used to describe both processes occurring without phase transitions and processes taking place in the presence of water-vapor transitions. The main difference between this approach and the theory employing a two-phase region lies in the method of closing the system of equations composed of conservation laws. In models with a two-phase region, the system is closed by the condition of thermodynamic equilibrium of the phases. In contrast to the models of phase transformation involving a temperature range, this approach not only makes it possible to avoid complex and time-consuming experiments for determination of the dependence of phase composition on the state parameters, but it also makes it unnecessary to calculate this dependence.

In the present study, we attempt to offer a physically consistent description of the process of vapor formation in a water-saturated porous medium within the framework of a model with a two-phase region.

1. Equations of Heat and Mass Transfer and Conditions at Discontinuities. The system of equations which describes heat and mass transfer in a porous medium saturated by a two-phase liquid is composed [6] of the equation of continuity of the mixture

$$\frac{\partial}{\partial t} [ms\rho_1 + m(1-s)\rho_2] + \nabla(\rho_1\mathbf{v}_1 + \rho_2\mathbf{v}_2) = 0, \quad (1)$$

the generalized filtration law for the  $i$ -th phase

$$\mathbf{v}_i = -\frac{k}{\mu_i} f_i(s) \nabla P, \quad i = 1, 2, \quad (2)$$

and the heat balance equation

$$\frac{\partial}{\partial t} [(1-m)\rho_s c_s T + ms\rho_1 e_1 + m(1-s)\rho_2 e_2] =$$

$$= \nabla \left( \Lambda \nabla T - \sum_{i=1}^2 \rho_i h_i v_i \right). \quad (3)$$

Equations (1-3) are valid if the functions in them are sufficiently smooth over the space variables. In the presence of discontinuities, system (1-3) must be augmented by balance conditions for mass, momentum, and energy at the discontinuities [7]. In the case of noninertial motion, these conditions have the form

$$\left[ \sum_{i=1}^2 m s_i \rho_i (D_i - D) \right]_{\pm}^{\pm} = 0, \quad (4)$$

$$[P]_{\pm}^{\pm} = 0, \quad (5)$$

$$\left[ \sum_{i=1}^2 m s_i \rho_i h_i (D_i - D) + Q_n \right]_{\pm}^{\pm} = 0, \quad (6)$$

where  $D$  and  $D_i$  are projections of the velocities of points of the surface of discontinuity and the particles of the  $i$ -th phase along a normal  $n$  to the surface of discontinuity;  $Q_n = -\Lambda(\nabla T)_n$  is the projection of the heat-flux vector on the normal  $n$ ;  $s_i$  is the saturation of the  $i$ -th phase;  $s_1 = s$ ,  $s_2 = 1 - s$ .

The presumption that the phases are in thermodynamic equilibrium leads to the auxiliary conditions

$$[T]_{\pm}^{\pm} = 0, \quad P_* = P_r(T_*). \quad (7)$$

In the region of the vapor-water mixture, system (1-3) is closed by the equation of state of the phases and the functional relation  $P = P_r(T)$ . The equations of state are sufficient to close system (1-3) in the frontal model.

2. Equations of State, Caloric Equations, and Thermophysical Parameters. We will use the indices 1 and 2 to denote quantities pertaining to the water and water vapor, respectively. We will use the following equations of state and caloric equation:

$$\rho_i = \rho_i^0 [1 + \alpha_i (P - P_a) - \beta_i (T - T_a)], \quad \rho_2 = P/(RT), \quad (8)$$

$$h_i = c_p^i T + h_i^0, \quad i = 1, 2, \quad (9)$$

where  $R$  is the universal gas constant.

With elastic strains of the medium, porosity is usually assumed to be equal to

$$m = m_a [1 + \alpha_s (P - P_a)]. \quad (10)$$

The dependence of  $\mu_i$ ,  $c_p^i$ ,  $\lambda_i$  and  $\lambda_s$  on temperature and pressure will henceforth be ignored.

We will use the following formulas for the phase permeabilities  $f_i(s)$

$$f_1(s) = \begin{cases} 0, & 0 \leq s \leq 0,2, \\ \left( \frac{s - 0,2}{0,8} \right)^{3,5}, & 0,2 \leq s \leq 1, \end{cases} \quad (11)$$

$$f_2(s) = \begin{cases} \left( 1 + 3s \left( \frac{0,9 - s}{0,9} \right)^{3,5} \right), & 0 \leq s \leq 0,9, \\ 0, & 0,9 \leq s \leq 1. \end{cases} \quad (12)$$

For the function  $P_r(T)$ , we will use an approximate expression which follows from the Clausius-Clapeyron equation:

$$P_r(T) = P_{\phi} \exp \left( \frac{B}{R} \ln \left( \frac{T}{T_{\phi}} \right) + \frac{A}{R} \left( \frac{1}{T_{\phi}} - \frac{1}{T} \right) \right), \quad (15)$$

where  $A$  and  $B$  are known constants;  $P_{\phi}$  and  $T_{\phi}$  are the pressure and temperature corresponding to a certain equilibrium state of the vapor-water system.

3. Transformation of the Heat and Mass Transfer Equations and the Conditions at Discontinuities. Let us subject Eqs. (1-3) to preliminary transformations. Using caloric equations (9) and excluding the vectors  $v_1$  and  $v_2$ , after some simple transformations we can reduce system (1-3) to the form:

$$\left[ \sum_{i=1}^2 s_i \left( \frac{dm}{dP} \rho_i + m \frac{\partial \rho_i}{\partial P} \right) \right] \frac{\partial P}{\partial t} + \left[ \sum_{i=1}^2 m s_i \frac{\partial \rho_i}{\partial T} \right] \frac{\partial T}{\partial t} + m(\rho_1 - \rho_2) \frac{\partial s}{\partial t} = \nabla(K_s \nabla P), \quad (16)$$

$$C \frac{\partial T}{\partial t} + m q \frac{\partial s}{\partial t} + \frac{\partial m P}{\partial t} = \nabla(\Lambda \nabla T + K_e \nabla P), \quad (17)$$

where

$$K_s = k \sum_{i=1}^2 f_i \rho_i / \mu_i, \quad K_e = k \sum_{i=1}^2 f_i \rho_i h_i / \mu_i;$$

$$C = (1 - m) \rho_s c_s + \sum_{i=1}^2 m s_i \rho_i c_p^i$$

is the effective heat capacity;  $q = \rho_1 h_1 - \rho_2 h_2$  is the heat of phase transformation.

In regions of the space  $s$ , system (16-17) reduces to a system of equations relative to  $P$  and  $T$ . In the region of the two-phase state, the number of unknowns decreases after substitution of the function  $P = P_r(T)$  into the equation and again becomes equal to two. However,  $s$  and  $T$  become unknowns in the latter case.

Let us transform the right sides of Eqs. (16-17):

$$\left[ \sum_{i=1}^2 s_i \left( \frac{dm}{dP} \rho_i + m \frac{\partial \rho_i}{\partial P} \right) \right] \frac{\partial P}{\partial t} + \left[ \sum_{i=1}^2 m s_i \frac{\partial \rho_i}{\partial T} \right] \frac{\partial T}{\partial t} + m(\rho_1 - \rho_2) \frac{\partial s}{\partial t} =$$

$$= \frac{\partial K_s}{\partial P} (\nabla P)^2 + \frac{\partial K_s}{\partial T} \nabla T \nabla P + \frac{\partial K_s}{\partial s} \nabla s \nabla P + K_s \Delta P,$$

$$C \frac{\partial T}{\partial t} + m q \frac{\partial s}{\partial t} + m \frac{\partial P}{\partial t} = m(\lambda_1 - \lambda_2) \nabla s \nabla T + \Lambda \Delta T +$$

$$+ \frac{\partial K_e}{\partial P} (\nabla P)^2 + \frac{\partial K_e}{\partial T} \nabla T \nabla P + \frac{\partial K_e}{\partial s} \nabla s \nabla P + K_e \Delta P. \quad (19)$$

In Eq. (19), we ignored the pressure dependence of porosity, since the energy contribution connected with this dependence is negligible compared to the incoming heat flow.

Let us examine system (18-19) in the regions of a one-phase state. Inserting the equation of state of the vapor into Eqs. (18-19) and assuming that  $s = 0$ , after performing some simple transformations we obtain the following for the system of equations in the vapor region

$$\frac{\mu_2}{k} \left( m_a \alpha_s + \frac{m}{P} \right) \frac{\partial P}{\partial t} - \frac{\mu_2 m}{k T} \frac{\partial T}{\partial t} = \frac{1}{P} (\nabla P)^2 - \frac{1}{T} \nabla T \nabla P + \Delta P, \quad (20)$$

$$C_2 \frac{\partial T}{\partial t} + m \frac{\partial P}{\partial t} = \Lambda_2 \Delta T + \frac{k c_p^2}{\mu_2 R} [(\nabla P)^2 + P \Delta P]. \quad (21)$$

Here,  $C_2 = (1 - m) \rho_s c_s + m \rho_2 c_2$ ,  $\Lambda_2 = (1 - m) \lambda_s + m \lambda_2$ . In Eqs. (10-21), we can ignore the relation  $m = m(P)$  and assume that  $m = \text{const} = m_a$ . Moreover, in actual porous media,  $\alpha_s \ll 1/P$ . Thus  $\alpha_s$  can be dropped from Eq. (20).

In the water region ( $s = 1$ ), we write Eqs. (18-19) as follows after we insert the equation of state of water

$$\frac{\mu_1}{k} \left( m_a \alpha_s + m \frac{\rho_1^a}{\rho_1} \alpha_1 \right) \frac{\partial P}{\partial t} - \frac{\mu_1 m \rho_1^a}{k \rho_1} \beta_1 \frac{\partial T}{\partial t} =$$

$$= \alpha_1 (\nabla P)^2 - \beta_1 \frac{\rho_1^a}{\rho_1} \nabla T \nabla P + \Delta P, \quad (22)$$

$$C_1 \frac{\partial T}{\partial t} + m \frac{\partial P}{\partial t} = \Lambda_1 \Delta T + T \frac{k}{\mu_1} \rho_1^a c_p^1 \alpha_1 (\nabla P)^2 + \quad (23)$$

$$+ \frac{k}{\mu_1} \rho_1 c_p^1 \left(1 - \frac{\rho_1^a}{\rho_1} \beta_1\right) \nabla T \nabla P + T \frac{k}{\mu_1} \rho_1 c_p^1 \Delta P,$$

where  $C_1 = (1 - m)\rho_S c_S + m\rho_1 c_p^1$ ;  $\Lambda_1 = (1 - m)\lambda_S + m\lambda_1$ . Equations (22) and (23) can be simplified by discarding the small terms:

$$\frac{\mu_1 m}{k} (\alpha_s + \alpha_1) \frac{\partial P}{\partial t} - \frac{\mu_1 m}{k} \beta_1 \frac{\partial T}{\partial t} = -\beta_1 \nabla T \nabla P + \Delta P, \quad (24)$$

$$C_1 \frac{\partial T}{\partial t} = \Lambda_1 \Delta T + \frac{k}{\mu_1} \rho_1 c_p^1 \nabla T \nabla P. \quad (25)$$

Here, the term  $\alpha_1 (\nabla P)^2$  was discarded in connection with its smallness. We also discarded terms connected with the work of the internal surface forces, and we put  $m = \text{const} = m_a$ .

Let us transform the mass- and heat-balance conditions at a discontinuity, using the generalized Darcy's law and conditions (5-7). We write the mass-balance condition for the surface of discontinuity in the form

$$\left[ \sum_{i=1}^2 m s_i \rho_i D_i \right]_{-}^{+} = \left[ \sum_{i=1}^2 m s_i \rho_i \right]_{-}^{+} D,$$

from which we obtain

$$- [K_s (\nabla P)_n]_{-}^{+} = m [s]_{-}^{+} (\rho_1^* - \rho_2^*) D. \quad (26)$$

We similarly transform the condition of heat balance at the discontinuity

$$- [K_e (\nabla P)_n]_{-}^{+} = m q [s]_{-}^{+} D + [\Lambda (\nabla T)_n]_{-}^{+}. \quad (27)$$

In the model with the two-phase region, we add the following equation to conditions (26-27)

$$(\nabla P)_n^- = P'_r (T_*) (\nabla T)_n^-. \quad (28)$$

4. Frontal Model and Model with Two-Phase Region in the Case of Unidimensional Processes. Let us examine a unidimensional vaporization process. Let  $P_0$  and  $T_0$  be the initial pressure and temperature and let them be constant at  $x > 0$ . Meanwhile,  $P_0 > P_r(T_0)$ :

$$P|_{t=0} = P_0, \quad T|_{t=0} = T_0. \quad (29)$$

We will assume that the following conditions hold on the boundary beginning with the moment of time  $t > 0$

$$\begin{cases} P|_{x=0} = P_1 < P_r(T_0), \\ T|_{x=0} = T_1. \end{cases} \quad (30)$$

We assign the conditions at infinity through the limiting relations

$$\lim_{x \rightarrow \infty} P = P_0, \quad \lim_{x \rightarrow \infty} T = T_0. \quad (31)$$

The frontal model and the model with a two-phase region permit similarity solutions in such a formulation. By making the substitution  $\xi = x/\sqrt{t}$ , we reduce Eqs. (18-21) and (24-25) to ordinary differential equations. The solutions of these equations in the transitional regions are combined by using the conditions for the discontinuities.

We will write out the conditions on the vaporization front

$$\frac{\rho_2^*}{\rho_1^*} \frac{k}{\mu_2} P'^- = \frac{k}{\mu_1} P'^+ + m \left(1 - \frac{\rho_2^*}{\rho_1^*}\right) \frac{\beta}{2}, \quad (32)$$

$$P_* = P^+ = P^- = P_r(T_*), \quad (33)$$

$$T_* = T^+ = T^-, \quad (34)$$

$$T'^- = \frac{k}{\mu_1 \Lambda_1} \rho_1^* h_1^* P'^+ - \frac{k}{\mu_2 \Lambda_2} \rho_2^* h_2^* P'^- + m q \frac{\beta}{2} + \frac{\Lambda_1}{\Lambda_2} T'^+, \quad (35)$$

where  $\beta$  is the similarity coordinate of the front.

Equations (20-21) and (24-25) take the form:

$$-\frac{\xi}{2} \frac{\mu_2 m}{k} \frac{P'}{P} + \frac{\xi}{2} \frac{\mu_2 m}{k} \frac{T'}{T} = \frac{(P')^2}{P} + P'' - \frac{T'}{T} P', \quad (36)$$

$$-\frac{\xi}{2} C_2 T' - \frac{\xi}{2} m P' = \Lambda_2 T'' + \frac{k c_p^2}{\mu_2 R} [(P')^2 + P P''], \quad (37)$$

for the vapor ( $0 \leq \xi \leq \beta$ ) and

$$-\frac{\xi}{2\kappa} P' + \frac{\xi}{2} \frac{\mu_2 m}{k} T' = P'' - \beta_1 T' P', \quad (38)$$

$$-\frac{\xi}{2a_1} T' = T'' + \frac{k \rho_1 c_p^1}{\mu_1 \Lambda_1} P' T', \quad (39)$$

for the water ( $\beta \leq \xi \leq \infty$ ). In the above equations,  $\kappa = k(\alpha_s + \alpha_1)^{-1}/(\mu_1 m)$  is piezoelectric conductivity;  $\alpha_1 = \Lambda_1/C_1$  is the diffusivity of the water-saturated porous medium.

We will use the following algorithm to solve the above problem numerically. We reduce system (36-39) to a first-order system and we choose four free parameters  $\beta$ ,  $T_*$ ,  $P'^+$ ,  $T'^+$ , which we will use to control the "trajectory" of the solution of the Cauchy problem in the liquid and vapor regions. In the vapor region, this problem is solved from right to left with the "initial" data  $P_*$ ,  $T_*$ ,  $P'^-$ ,  $T'^-$ , where  $P'^-$  and  $T'^-$  are found from conditions (32-35). The free parameters are varied until the boundary conditions are satisfied at infinity and at  $\xi = 0$ .

In the model with the two-phase region, the entire numerical axis  $x > 0$  is generally represented by three intervals: the vapor region  $0 \leq x \leq X_1$ ; the two-phase region  $X_1 \leq x \leq X_2$ ; the water region  $X_2 \leq x < \infty$ . We use  $\gamma$  and  $\beta$  to represent the similarity coordinates of the boundary of the two-phase region ( $\gamma < \beta$ ). The equations of the frontal model (36-39) remain valid in the vapor and water regions. In the two-phase region, we additionally use Eqs. (18-19) (the changeover to the similarity variable in these equations is quite simple and is not discussed here). At the boundaries of the two-phase region, saturation  $s$  is generally discontinuous. At the forward boundary ( $\xi = \beta$ ), saturation undergoes the discontinuity

$$s^+ = 1, \quad s^- = s^*, \quad (40)$$

where  $s^*$  is the sought value. We write out the conditions for  $\beta$ :

$$-(K_s^+ P'^+ - K_s^- P'^-) = m(1 - s^*)(\rho_1^* - \rho_2^*) \frac{\beta}{2}, \quad (41)$$

$$-(K_e^+ P'^+ - K_e^- P'^-) = m q (1 - s^*) \frac{\beta}{2} + \Lambda^+ T'^+ - \Lambda^- T'^-, \quad (42)$$

$$P_\beta = P^+ = P^-, \quad P_\beta = P_r(T_\beta), \quad (43)$$

$$T_\beta = T^+ = T^-, \quad (44)$$

$$P'^- = P'_r(T_\beta) T'^-. \quad (45)$$

On the boundary  $\xi = \gamma$ , saturation is continuous and decreases to zero:  $s^+ = s^- = 0$ . It follows from Eqs. (4-6) at  $\xi = \gamma$  that

$$T^+ = T^- = T_\gamma, \quad P^+ = P^- = P_r(T_\gamma), \quad T'^+ = T'^-, \quad P'^+ = P'^-. \quad (46)$$

We will use the following scheme to solve the model with the two-phase region. Proceeding as we did in the frontal model, we construct the solution in the liquid phase  $\beta \leq \xi < \infty$ , choosing four free parameters  $\beta$ ,  $T_\beta$ ,  $P'^+$ ,  $T'^+$ . Inserting condition (45) into the mass- and heat-balance conditions (40-41), we find the values of  $s^*$  and  $T'^-$ . Here, the latter two quantities are expressed through already-known variables with the index +. Since Eqs. (18-19) are of the first order relative to  $s$ , knowledge of the values of  $s^*$ ,  $T$ , and  $T'^-$  is sufficient to solve the Cauchy problem to the left of  $\beta$ . (We remind the reader that we substituted the relation  $P = P_r(T)$  into Eqs. (18-19).) In the process of solving the Cauchy problem, we find the point  $\gamma$  at which  $s(\gamma) = 0$ . The solution is then continued smoothly

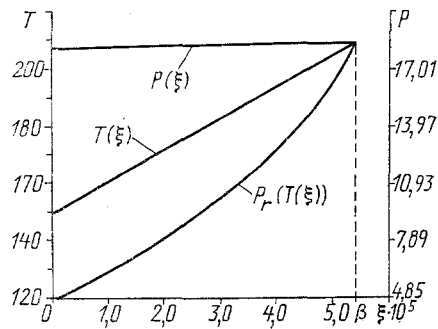


Fig. 1. Supercooling of vapor in a uni-dimensional frontal model,  $P_0 = 80$  atm,  $P_1 = 4.85$  atm,  $T_0 = 215^\circ\text{C}$ .  $T$ ,  $^\circ\text{C}$ ;  $P$ , atm;  $\xi$ ,  $\text{m}/\sqrt{\text{sec}}$ .

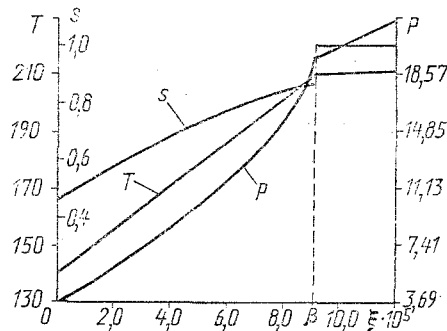


Fig. 2. Unidimensional model with two-phase region: case of a solution with a two-zone structure,  $P_0 = 60$  atm,  $P_1 = 3.69$  atm,  $T_0 = 215^\circ\text{C}$ .

into the vapor region with conditions (46). The free parameters are varied until the boundary conditions are satisfied at  $\xi = 0$  and  $\xi \rightarrow \infty$ .

We used a variant of the Runge-Kutta method with fourth-order accuracy to perform the calculations. The step was selected automatically in this variant. Certain complications connected with loss of stability of the Cauchy problem as the boundary  $\xi = 0$  was approached were encountered in the numerical calculation. As was shown by subsequent calculations, this instability was due to the presence of a thermal boundary layer in the neighborhood of the boundary  $\xi = 0$ . The computational difficulties were resolved by extending the scale in the boundary region. It is natural to expect the presence of a thermal boundary layer to cause  $\beta$  to be slightly dependent on the temperature boundary condition at  $\xi = 0$ . This is in fact the situation we observed in our numerical calculation.

The calculations provided evidence of the physical contradiction of the frontal model for actual porous media having permeabilities no less than  $10^{-16}$   $\text{m}^2$ . The contradiction lies in the manifestation of "supercooling" of the vapor and/or "superheating" of the water. The frontal regime may be realized at lower permeabilities (such as in clays). Figure 1 illustrates the case of supercooling of vapor in the frontal model. The three-zone structure of the solution in the model with the two-phase region is seen at permeabilities close to the permeability of clays. At lower  $k$ , only a two-zone structure (water-vapor mixture and water) is realized (see Fig. 2).

The model constructed here can be used to analyze processes which take place in high-temperature strata containing geothermal water.

We used the following initial data in our calculations:  $m = 0.25$ ,  $\rho_1 = 10^3$   $\text{kg}/\text{m}^3$ ,  $\rho_S = 2.6 \cdot 10^3$   $\text{kg}/\text{m}^3$ ,  $k = 10^{-11} - 10^{-17}$   $\text{m}^2$ ,  $\mu_1 = 0.001$   $\text{Pa} \cdot \text{sec}$ ,  $\mu_2 = 1.22 \cdot 10^{-5}$   $\text{Pa} \cdot \text{sec}$ ,  $c_p^1 = \text{J}/\text{kg}/\text{K}$ ,  $c_p^2 = 2000$   $\text{J}/\text{kg}/\text{K}$ ,  $c_S = 840$   $\text{J}/\text{kg}/\text{K}$ ,  $\lambda_1 = 0.682$   $\text{W}/\text{m}/\text{K}$ ,  $\lambda_2 = 0.03$   $\text{W}/\text{m}/\text{K}$ ,  $\lambda_S = 1.0$   $\text{W}/\text{m}/\text{K}$ ,  $\alpha_1 = 0.5 \cdot 10^{-9}$   $\text{Pa}^{-1}$ ,  $\alpha_S = 10^{-10}$   $\text{Pa}^{-1}$ ,  $P_\phi = 15.9 \cdot 10^5$   $\text{Pa}$ ,  $T_\phi = 473$   $\text{K}$ ,  $A = 3.1412 \cdot 10^6$   $\text{J}/\text{kg}$ ,  $B = -2,3446 \cdot 10^3$   $\text{J}/\text{kg}/\text{K}$ .

## NOTATION

$m$ , porosity;  $s$ , water saturation;  $\rho_i$ , density;  $v_i$ , filtration velocity;  $k$ , absolute permeability;  $f_i$ , relative permeability;  $\mu_i$ , viscosity;  $e_i$ , specific energy;  $h_i$ , specific heat;  $\alpha_1$ , coefficient of compressibility of water;  $\beta_1$ , coefficient of thermal expansion of water;  $\alpha_s$ , elastic modulus of skeleton;  $\lambda_i$ , thermal conductivity of the  $i$ -th phase;  $\Lambda$ , effective thermal conductivity of the mixture;  $P = P_r(T)$ , saturation vapor pressure at the given temperature;  $c_p^i$ , isobaric heat capacity of the  $i$ -th phase;  $c_s$ , heat capacity of the skeleton;  $\rho_i^*$ , density at a discontinuity. Indices: 1) water; 2) vapor.

## LITERATURE CITED

1. V. T. Borisov, Dokl. Akad. Nauk SSSR, 136, No. 3, 583-586 (1961).
2. L. Rubinstein, "Free boundary problems: theory and applications," Research Notes in Mathematics, 78, 275-282 (1983).
3. V. M. Entov, A. M. Maksimov, and G. G. Tsypkin, Dokl. Akad. Nauk SSSR, 288, No. 3, 621-624 (1986).
4. A. V. Lykov, Theory of Drying [in Russian], Moscow-Leningrad (1950).
5. L. I. Heifitz and A. V. Neumark, Multiphase Processes in Porous Media [Russian translation], Moscow (1982).
6. G. I. Barenblatt, V. M. Entov, and V. M. Ryzhik, Motion of Liquids and Gases in Natural Reservoirs, Moscow (1984).
7. L. I. Sedov, Continuum Mechanics [in Russian], Vol. 1, Moscow (1970).

## CHANGE IN BOILING REGIMES ON THICK HEATING SURFACES

V. U. Sidyganov and E. V. Ametistov

UDC 536.423

An analysis is made of the dependence of the structure and velocity of the boiling-regime transition front on the level of heat release and the properties of a heating surface.

Changes in boiling regimes on heating surfaces are an important engineering problem. Solving this problem will make it possible to improve the efficiency of processes involving quenching and thermal stabilization and increase the reliability of steam generators, heat exchangers, and other heat-engineering apparatus. The dynamics of the regime transition determines the design response time for the protection of superconducting devices and the structure and properties of materials that are quenched.

There are presently two approaches to the study of boiling-regime changes. The first approach focuses on hydrodynamic and heat-transfer conditions in the vapor-liquid layer. The characteristic scales and times of these processes are determined by growing bubbles and jets of vapor which displace the liquid and wet the heating surface with drops of the liquid. The dynamics of other small hydrodynamic structures [1] also play a role in determining the characteristic scales and times [1]. The thermal perturbations generated by these structures penetrate the heating surface to a certain depth, so that the inertial thermal properties of the material of the surface affect the rate of heat transfer and the critical thermal loads [2].

In the second approach, the evolution of the temperature fields inside the heat-emitting surface is regarded as a very slow process which determines the dynamics of the boiling-regime shift [3]. Here, it is assumed that the Nukiyami boiling curve is externally assigned, either on the basis of an experiment or in accordance with some semi-empirical theory developed by the first approach. The evolution of the temperature fields should occur at scales greater than the size of the small nonsteady hydrodynamic structures mentioned above.